www.vbripress.com/aml, DOI: 10.5185/amlett.2016.6433

Copper oxide nano-particles film on glass by using sputter and chemical bath deposition technique

Avishek Das[1,2], Ajay Kushwaha[1], Nakul Raj Bansal[1], Vignesh Suresh[1], Sanghamitra Dinda[1], Sanatan Chattopadhyay[2,3*], Goutam Kumar Dalapati[1*]

[1]*Institute of Materials Research and Engineering, A*STAR (Agency for Science, Technology and Research),*
2 Fusionopolis Way, #08-03, Innovis, 13863, Singapore
[2]*Department of Electronic Science, University of Calcutta, 92-A. P. C. Road, Kolkata 70000, India*
[3]*Centre for Research in Nanoscience and Nanotechnology (CRNN), University of Calcutta,*
JD-2 Sector III, Kolkata 700098, India

[*]Corresponding author. E-mail: dalapatig@imre.a-star.edu.sg

Received: 16 January 2016, Revised: 20 April 2016 and Accepted: 22 May 2016

ABSTRACT

In the present work, cupric oxide (CuO) nanoparticle (NP) thin films were synthesized on glass by combination of sputter and chemical bath deposition technique. The CuO seeds were deposited by using radio frequency (RF) sputter technique at room temperature. CuO nanoparticles were prepared by chemical bath deposition. Effect of solute molar concentration (0.02 to 0.04M) and annealing temperature (at 400°C) on nanoparticles size and distribution were studied. The average size of nanoparticles is small in lower molar concentration, which is restructured after annealing to form dense film with relative smaller size nanoparticles. The work opens up new route to synthesize CuO nanorticle thin films for different applications. Copyright © 2016 VBRI Press.

Keywords: CuO; R.F. sputter; chemical bath deposition; nanoparticle thin film.

Introduction

Semiconductor metal oxides have attracted a great deal of interest for many decades due to their potential physical and chemical properties. Among all other metal oxides, copper oxide has gained much scientific attention for its non-toxic and abundant component elements. Cuprous oxide (or copper (I) oxide) and cupric oxide (or copper (II) oxide) are the two main forms of Copper oxide. Cuprous oxide (Cu_2O) has direct-bandgap energy of ~2.1 eV and is a good choice for applications in the field of photocatalytic and photoelectrocatalysis water splitting [**1, 2**]. Whereas Cupric oxide (CuO) being p-type semiconductor with a bandgap of ~1.5 eV, with high optical absorption, abundance, and non-toxicity is a suitable candidate for solar cell applications [3-7]. Recently, *Masudy-Panah et al.* reported highest efficiency of more than 1% for p-CuO/n-Si heterojunction based solar cells [**8-9**]. Several synthesis techniques are available for the CuO nanoparticles such as Sol-gel, precipitation, thermal oxidation and microwave assisted solvothermal method [**10-12**]. Due to the high surface to volume ratio, nanoparticle based thin films can be used as the material for solar energy harvesting. Therefore, it is worthy to develop an effective way to produce high quality CuO nanoparticle based thin films in large scale for device fabrication. The sputter deposition technique has been used to deposit high quality thin films for solar cells application [**13-21**].

In this work, a recipe to fabricate highly populated and uniform CuO nanoparticle based thin film has been proposed with combined sputter and chemical bath deposition approaches. The template for CuO nanoparticle was deposited by employing sputtering technique which enhanced the density and uniformity of CBD grown CuO nanoparticle distribution over the substrate. Effects of solute molar concentration and post annealing have been studied.

Experimental

Synthesis of CuO nano-particle thin film

For the growth of copper oxide nanostructured thin films, standard borofloat glasses were used as substrates. Prior to deposition, the substrates were cleaned sequentially with trichloroethylene, acetone, isopropyl alcohol and de-ionized water under continuous ultrasonication for 5 minutes, to remove any metal and organic contaminations and were dried by blowing Nitrogen gas before loading into the chamber. The CuO nanostructures were grown by two-step method. At first, CuO nanoseeds were prepared by RF sputtering with a stoichiometric copper oxide target on borofloat glass slides as the substrates. For the removal of surface oxide layer from the target, the target was pre-sputtered in argon atmosphere for 5 minutes. CuO was sputtered at a pressure of 3.3mTorr with 24.9 sccm argon gas flow. The deposition was carried out for 5 minute with r.f. power of 50W, keeping substrates at room temperature.

For the growth of CuO nanostructures, chemical bath deposition method was employed, where equi-molar aqueous solutions of 0.02M, 0.03M and 0.04M Copper (II) Nitrate Trihydrate [$Cu(NO_3)_2.3H_2O$] and Hexamethylenetetramine ($C_6H_{12}N_4$, HTMA) in de-ionized water were prepared. The seed coated samples were dipped vertically into the solution under constant stirring. The bath solution was kept in atmospheric pressure at a controlled temperature of 90^oC and deposition was carried out for 50 minutes. After deposition, the samples were taken out and washed with running de-ionized water to remove the residual solutes and impurities and were dried by blowing nitrogen gas. The grown samples were annealed at 400^0C for 1 hour.

Structural and crystallographic measurements of CuO nano-particle thin film

The surface morphology and its micro-structure were analyzed by FESEM (JEOL FESEM JSM 6700F). Crystalline structural was studied by X-Ray Diffraction (XRD) using a Bruker AXS General Area Detector Diffraction System (GADDS) with CuKα (λ = 0.15418 nm) radiation.

Results and discussion

The chemical bath contains an aqueous solution of Copper (II) Nitrate Trihydrate and Hexamethylenetetramine (HTMA) which provides the required NH_4^+ and OH^- ions by its thermal decomposition. Chemical reaction and growth of CuO during the deposition is given below [**22**].

$$C_6H_{12}N_4 + 2(3H_2O) \rightarrow 6CH_2O + 4NH_3$$
$$NH_3 + H_2O \rightarrow NH_4^+ + OH^-$$

NH_4^+ react with copper nitrate to form ammonium nitrate $NH_4(NO_3)$ and copper hydroxide $Cu(OH)_2$. With increase in bath temperature and time, this intermediate growth of $Cu(OH)_2$ is converted to solid phase CuO by dehydration reaction.

$$Cu(NO_3)_2 + 2NH_4^+ + 2OH^- \rightarrow 2NH_4(NO_3) + Cu(OH)_2$$
$$Cu^{2+} + 2OH^- + 2H_2O \rightarrow Cu\,(OH)_4^{2-} + 2H^+$$
$$Cu\,(OH)_4^{2-} + 2H^+ \rightarrow CuO^{Solid} + 3H_2O$$

The $Cu(OH)_2$ does not fully dehydrate at this relatively low temperature of 90^oC and its presence can be observed in the XRD pattern for as deposited samples in **Fig. 3(a)**. However, during annealing the residual $Cu(OH)_2$ converts to CuO by releasing water molecule in form of vapor, as reported by *Shinde et al* for textured ZnO films [**23**].

$$Cu\,(OH)_2 \leftrightarrow Cu^{2+} + 2[O^- + H^+] \leftrightarrow CuO^{Solid} + H_2O^{Vapor}$$

The FESEM images of as deposited and annealed samples are shown in **Fig. 1**. It is evident from FESEM images that the growth of CuO nano-particle thin film is very dense on the substrate for all the molar concentrations considered. **Fig. 1(a), (b)** and **(c)** represents CuO nano-particle for the molar concentrations of 0.04M, 0.03M and 0.02M of solutes. With decreasing molar concentration of both the solutes, the as-deposited particle size seems to be decreasing and this is also observed for the samples after annealing at 400^0C for 1 hour. Average thickness of all the grown film was observed to be ~100nm. The morphology of grown nanoparticles for as deposited samples was observed to be changing from arbitrary to confined shape with decrease in molar concentration of the solutes. Whereas, the observed morphology for all the annealed samples were well confined. The size of the CuO nanoparticles decreased after annealing as depicted in **Fig. 1**.

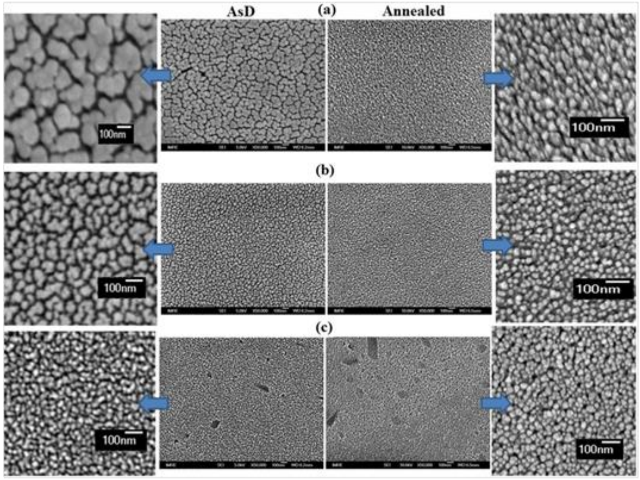

Fig. 1. SEM image of CuO the nanoparticle thin film for as-deposited (Left side) annealed sample (right side) for (a) 0.04M, (b) 0.03M and (c) 0.02M bath solution.

Moreover, the morphology of such nanoparticle film becomes increasingly spherical. The grain boundary begins to fade away and the NPs fuse together in the process of forming homogenous thin film. The islets of CuO formed during the deposition, come closer together and thereby merge the grain boundaries resulting in a more homogenous morphology. To study the effect of molar concentration on the morphology, average particle diameter was measured and based on histogram analysis, Gaussian fitted distribution curves are plotted in **Fig.2 (a)** and **(b)**.

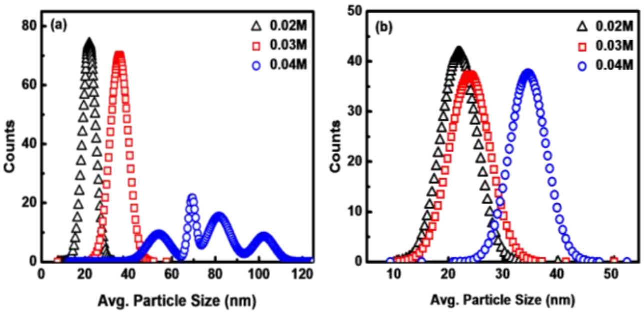

Fig. 2. Average particle size Gaussian distribution of (a) as deposited and (b) annealed sample for different molar concentrations of the solutes.

The average particle size for the as-deposited 0.04 M sample is not uniform throughout and has multiple distribution peaks within 50 – 100 nm. Whereas, the distribution is very sharp for 0.03 M and 0.02 M samples, centered at ~36 nm and ~22nm. The average particle size for annealed samples shows sharp Gaussian distributions, centered at ~35nm, ~24nm and ~22nm for 0.04M, 0.03M and 0.02M samples. It is interesting to note that annealing also plays a major role in defining the particle geometry. The particle size is observed to decrease with annealing and its morphology is becoming more spherical. This effect is believed to be due to the detachment of two or more fused CuO nanoparticles. The variations in size for the as-deposited nano-particle sample of 0.04M concentration may be attributed to the fusion of two or more CuO nanoparticles with each other randomly. The separation of fused nanoparticles after annealing may also be attributed to the removal of Cu(OH)2 from the CuO crystals. X-ray diffraction patterns obtained for as deposited as well as annealed samples are depicted in **Fig. 3 (a)** and **(b)**, respectively. Black, red and blue solid lines represent the XRD patterns for 0.02, 0.03 and 0.04M of the solute concentrations, respectively. Among three different samples, 0.04M grown sample shows the most significant diffraction peaks for (110), (002)/(-111), (111) and (020) planes for as-deposited and annealed conditions. Similar peaks also were observed for the sputter deposited CuO as reported in [**24-26**].

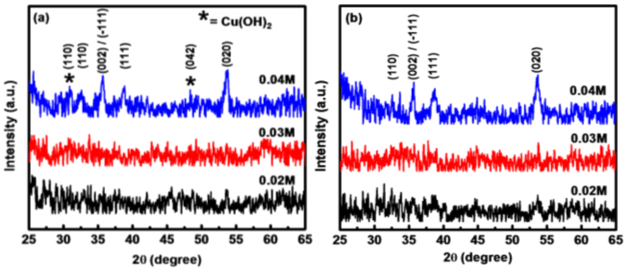

Fig. 3. XRD pattern for (a) as deposited and (b) annealed sample of 0.02M, 0.03M and 0.04M.

This may be attributed to large grain size of the CuO nanoparticle which is also relevant with the SEM image for 0.04M sample in **Fig. 1(a)** and **(b)**. The degradation and noise in the diffraction intensity is expected due to the low thickness of grown nanoparticle thin film, XRD peaks of the samples confirm the growth of CuO with monoclinic crystal structure with their appropriate resemblance with the CuO JCPDS card no-80-1268.The relatively broader peaks appear from the smaller grain size which is also consistent with the SEM images of **Fig. 1** and Gaussian distributions of **Fig. 2 (a)** and **(b)**. Apart from the XRD peaks of as deposited CuO, there are also few low intensity peaks for $Cu(OH)_2$ observed which agrees with JCPDS card no-80-0656 for orthorhombic $Cu(OH)_2$. According to the figure 3(b), most of the hydroxides have been converted into oxides during annealing. However, a little residue is observed in the diffraction peaks for hydroxide. Nevertheless, the conversion factor is very significant and the intensity of hydroxide significantly drops after annealing. Surface morphology of the sputter/CBD grown CuO nanostructure was shown in **Fig. 4**. The sputter/CBD grown CuO is homogenous over large areas as shown in the AFM. The Surface roughness of the thin films spanning an area of 5μm^2 for the samples obtained from 0.04M, 0.03M and 0.02 M bath solutions are 3.27nm, 3.3nm and 3.61nm, respectively.

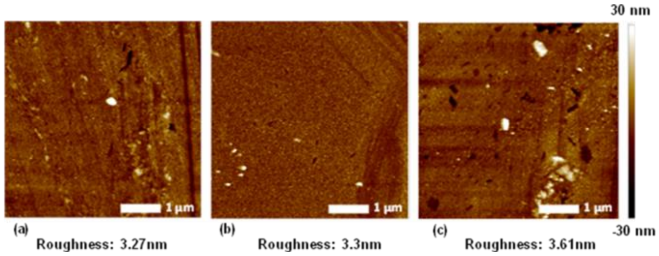

Fig. 4. Surface morphology of CuO nanoparticle thin film for (a) 0.04M, (b) 0.03M and (c) 0.02M bath solution.

Conclusion

CuO nanoparticle thin film was synthesized on borofloat glass by combination of sputter and chemical bath deposition technique. CuO seeds were deposited by R.F. sputter and nanoparticles were prepared by chemical bath deposition with varying molar concentration of solutes. The prepared samples were annealed at 400^{0}C for 1 hour. Grown and annealed samples are CuO with monoclinic crystal structure. The average particle size decreases ~50-100nm, ~36 nm and ~22nm with decreasing solute molar concentration from 0.04M to 0.02M. Moreover, with annealing, particle size reduces further to ~35nm, ~24nm and ~22nm for corresponding decrease in molar concentrations, respectively. Present work showed combined growth technique can be employed to grow highly dense and uniform CuO nanoparticle thin film for potential applications in solar energy harvesting application.

Acknowledgements

Avishek Das likes to acknowledge the Institute of Materials Research and Engineering (IMRE), A*STAR, Singapore and University Grants Commission (UGC), India for providing financial support to pursue his research.

Author contributions

Conceived the plan: G.K.D.; Performed the synthesis experiments: A.D., A.K.; N. B.; Data analysis: A.D.; V.S.; S.D.; G.K.D.; S.C.; Wrote the paper: A.D., S.C., G.K.D. Authors have no competing financial interests.

Reference

1. Somasundaram, S.; Chenthamarakshan, C. R. N.; de Tacconi, N. R.; Rajeshwar, K; *Int. J. Hydrogen Energy*, **2007**, 32, 4661.
   DOI: 10.1016/j.ijhydene.2007.06.028
2. Siripala, W.; Ivanovskaya, A.; Jaramillo, T. F.; Baeck, S. H.; McFarland, E. W.; *Sol. Energ. Mat. Sol. Cells*, **2003**, 77, 229.
   DOI:10.1016/S0927-0248(02)00343-4
3. Xia, Y.; Pu, X.; Liu, J.; Liang, J.; Liu, P.; Li, X.; Yu, X.; *J. Mater. Chem. A*, **2014**, 2, 6796.
   DOI: 10.1039/C4TA00097H
4. Dalapati, G. K.; Kajen, R. S.; Masudy-Panah, S.; Sonar, P.; *J. Phys. D: Appl. Phys.*,**2015**, 48, 495104.
   DOI: 10.1088/0022-3727/48/49/495104
5. Masudy-Panah, S.; Kumar, V.; Tan, C. C.; Radhakrishnan, K.; Chi, D. Z.; Dalapati, G. K.; *Proceedings of the IEEE 5th International Nanoelectronics Conference (INEC '13)*,**2013**, 378.
   DOI: 10.1109/INEC.2013.6466052
6. Kumar, V.; Masudy-Panah, S.; Tan, C. C.; Wong, T. K. S.; Chi, D. Z.; Dalapati, G. K.; *Proceedings of the IEEE 5th International Nanoelectronics Conference (INEC '13)*, **2013**, 443.

DOI: 10.1109/INEC.2013.6466072

7. Wong, T.K.S.; Zhuk, S.; Masudy-Panah, S.; Dalapati, G.K.; *Materials*, **2016**, 9, 271.
DOI: 10.3390/ma9040271
8. Masudy-Panah, S.; Radhakrishnan, K.; Tan, H. R.; Yi, R.; Wong, T. I.; Dalapati, G. K.; Sol. *Energy Mater. Sol. Cells.*, **2015**, 140, 266.
DOI: 10.1016/j.solmat.2015.04.024
9. Masudy-Panah, S.; Dalapati, G.K.; Radhakrishnan, K.; Kumar, A.; Tan, H.R.; Naveen Kumar, E.; Vijila, C.; Tan, C.C.; Chi, D.; *Prog. Photovoltaics Res. Appl.*,**2015**, 23, 637.
DOI: 10.1002/pip.2483
10. Usha, V.; Kalyanaraman, S.; Thangavel, R.; Vettumperumal, R.; *Superlattices Microstruct*., **2015**, 86, 203.
DOI: 10.1016/j.spmi.2015.07.053
11. Sahooli, M.; Sabbaghi, S.; Saboori, R.; *Mater. Lett*., **2012**, 81, 169.
DOI: 10.1016/j.matlet.2012.04.148
12. Rejith, S. G.; Krishnan, C.; *Mater. Lett*., **2013**, 106, 87.
DOI: 10.1016/j.matlet.2013.04.108
13. Dalapati, G.K.; Batabyal, S.K.; Masudy-Panah, S.; Su, Z.; Kushwaha, A.; Wong, T.I.; Liu, H.F.; Bhat, T.; Iskander, A.; Lim, Y.F.; Wong, L.H.; Tripathy, S.; Chi, D.; *Mater. Lett*. **2015**. 160, 45.
DOI: 10.1016/j.matlet.2015.07.089
14. Dalapati, G.K.; Tan, C.C.; Masudy-Panah, S.; Tan, H.R.; Chi, D.; *Mater. Lett.***2015**, 159, 455.
DOI: 10.1016/j.matlet.2015.07.066
15. Dalapati, G.K.; Liew, S.L.; Wong, A.S.W.; Chai, Y.; Chiam, S.Y.; Chi, D.Z.; *Appl. Phys. Lett*. **2011**, 98, 013507.
DOI: 10.1063/1.3536523
16. Kumar, A.; Dalapati, G.K.; Hidayat, H.; Law, F.; Tan, H.R.; Widenborg, P.I.; Hoex, B.; Tan, C.C.; Chi, D.Z.; Aberle, A.G.; *RSC Adv.***2013**, 3, 7733.
DOI: 10.1039/C3RA41156G
17. Dalapati, G.K.; Kumar, A.; Tan, C.C.; Liew, S.L.; Sonar, P.; Seng, H.L.; Hui, H.K.; Tripathy, S.; Chi, D.; *ACS Appl. Mater. Interfaces* **2013**, 5, 5455.
DOI: 10.1021/am400434q
18. Tan, C.C.; Dalapati, G.K.; Tan, H.R.; Bosman, M.; Hui, H.K.; Tripathy, S.; Chi, D.; *Cryst. Growth Des*. **2015**, 15, 1692.
DOI: 10.1021/cg501689d
19. Vaseem, M.; Umar, A.; Kim, S.H.; Hahn, Y.B.; *J. Phys. Chem. C*, **2008**, 112, 5729.
DOI: 10.1021/jp710358j
20. Dalapati, G.K.; Masudy-Panah, S.; Kumar, A.; Tan, C.C; Tan, H.R.; Chi, D.Z.; *Sci. Rep*.**2015**, 5, 17810.
DOI: 10.1038/srep17810
21. Masudy-Panah, S.; Moakhar, R.S.; Chua, C.S.; Tan, H.R.; Wong, T.I.; Chi, D.Z.; Dalapati, G.K.; *ACS Appl Mater. Interfaces***2016**,
DOI: 10.1021/acsami.5b09613
22. Dalapati, G.K.; Masudy-Panah, S.; Chua, S.T.; Sharma, M.; Wong, T.I.; Tan, H.R.; Chi, D.Z.; *Sci. Rep.***2016**, 6,20182,
DOI: 10.1038/srep20182
23. Shinde, V.R.; Lokhande, C.D.; Mane, R.S.; Han, S.H.; *Appl. Surf. Sci*., **2005**, 245, 407.
DOI: 10.1016/j.apsusc.2004.10.036
24. Masudy-Panah, S.; Dalapati, G.K.; Radhakrishnan, K.; Kumar, A.; Tan, H.R.; *J. Appl. Phys*., **2014**, 116, 074501.
DOI: 10.1063/1.4893321
25. Masudy-Panah, S; Radhakrishnan, K.; Kumar, A.; Wong, T.I.; Yi, R.; Dalapati, G.K.; *J. Appl. Phys*.,**2015,** 118, 225301.
DOI: 10.1063/1.4936318
26. Masudy-Panah, S; Moakhar R.S.; Chua, C.S.; Kushwaha, A.; Wong, T.I.; Dalapati, G.K.; *RSC Adv.*,**2016**, 6, 29383.
DOI: 10.1039/c6ra03383k